Fermilab Library
0 1160 0036163 8

DFUB 93-4
July 1993

FRAGMENTATION CROSS SECTIONS AND SEARCH FOR NUCLEAR FRAGMENTS WITH FRACTIONAL CHARGE IN RELATIVISTIC HEAVY ION COLLISIONS

S. Cecchini[2,3], H. Dekhissi,[1,2*], G. Giacomelli[1,2], G. Mandrioli[1,2], A. R. Margiotta[1,2], L. Patrizii[1,2], F. Predieri[1,2], P. Serra[1,2] and M. Spurio[1,2]

1) Dipartimento di Fisica dell' Universita' di Bologna, v. Irnerio 46, Bologna - Italy

2) INFN, Sezione di Bologna, v. Irnerio 46, Bologna - Italy

3) CNR- Istituto TESRE, v. de' Castagnoli 1, Bologna - Italy

AUG 0 199

Submitted to Astroparticle Physics

ABSTRACT

We present measurements of fragmentation cross sections of relativistic nuclei and upper limits for the production probability of nuclear fragments with fractional charge using CR39 nuclear track detectors and an automated scanning system.

The measurements of the total and partial charge changing fragmentation cross sections concern 16 GeV/nucleon oxygen ions, 14.5 GeV/nucleon silicon ions and 200 GeV/nucleon sulphur ions interacting in copper and CR39 targets.

No evidence for fractionally charged fragments was found requiring a minimum track length of 7 mm in CR39 detectors placed after a 14 mm copper target. The combined upper limit for the production probability of fractionally charged fragments relative to ordinary ones is at the level of $1.2\text{-}2.3\times10^{-4}$ (90% C.L.). The charge resolution of the CR39 detectors for an average of 10 measurements of the same track is $\sigma=0.05e$ at $Z=6$.

* Also Faculty of Science, University Mohamed I, Oujda, Morocco

1. INTRODUCTION

In this paper we present new measurements of fragmentation cross sections of high energy nuclei in CR39 and copper targets; we also present a search for nuclear fragments with fractional charges.

The fragmentation cross section of relativistic nuclei is important for nuclear physics and for interpreting observations in cosmic ray physics and astrophysics [1,2]. For instance they are needed to evaluate the changes in composition undergone by cosmic ray particles because of collisions with the interstellar medium. In particular, the cross sections in hydrogen are of high interest; they may be determined from the cross sections on polymers and higher Z nuclei using appropriate combinations [3].

The measurements of the nuclear breakup cross sections concern projectile nuclei of charge Z_j (j=8, 14, 16) in CR39 and copper targets to yield a nuclear fragment of charge Z_i, with $Z_i \geq 7$. We used the nuclear detector technique with the CR39 polymer, which has a threshold at about Z_t=5.

Nuclear track detectors, in particular the CR39 polymer ($C_{12}H_{18}O_7$), are capable of yielding precise measurements of the restricted energy loss of ionizing particles. This arises from the relatively low energy required to break polymeric bonds and because Landau fluctuations due to high energy δ-electrons do not contribute to the latent track formation. The radiation damage along the path of a particle may be developed to a microscope-visible cone by chemical etching.

We used CR39 nuclear track detectors made in collaboration with the Intercast Europe Co. (Parma, Italy). These are also employed as passive detectors in the MACRO experiment at the Gran Sasso underground Laboratory [4].

Stacks of CR39 detectors were exposed to relativistic heavy ions at the Brookhaven AGS and at the CERN SPS with the purposes of calibrating the CR39, of measuring the fragmentation cross sections and of searching for fractionally charged nuclei [5]. We measured with an automatic system about 160000 primary ions and 40000 nuclear fragments produced in the interactions of the beam particles in a copper target and in the CR39 itself. We obtained an average charge resolution σ=0.16e for one surface measurement and σ=0.05e at Z=6 for an average of 10 surface measurements of the same track.

Taking advantage of the extraordinary charge resolution of CR39, we searched for nonintegrally charged nuclear fragments. De Rujula et al., [6], Chapline [7] and Arbuzov [8] suggested that fragments with fractional charge might be formed in high energy nucleus-nucleus collisions by binding a free quark to nuclei containing 10 to 20 nucleons when a center of mass energy of about 2 GeV/nucleon is reached. No nuclear fragment with fractional charge was found. We estimate a combined upper limit of $1.2\text{-}2.3\times10^{-4}$ (90% Confidence Level, C.L.) for the production of fractionally charged fragments relative to ordinary ones in the collisions of 200 GeV/nucleon S nuclei, 14.5 GeV/nucleon Si nuclei and 16 GeV/nucleon O nuclei in copper.

In the following, after a brief recollection of the experimental method, we discuss the search for fractionally charged fragments and the measurements of the fragmentation cross sections in CR39 and in copper.

2. EXPERIMENTAL

The CR39 nuclear track detectors were made in collaboration with the Intercast Europe Company of Parma, Italy, using a custom made scientific line of production. Stacks of CR39 sheets were exposed at the Brookhaven AGS to 16 GeV/nucleon $^{16}O^{8+}$ ions in June 1988, to 14.5 GeV/nucleon $^{28}Si^{14+}$ ions in June 1990, and at the CERN SPS to 200 GeV/nucleon $^{32}S^{16+}$ ions in July 1990. In these exposures we managed to keep the ion density in the sheets to about 1500 ions/cm^2. Each CR39 sheet had a size of 13x7 cm^2 and was 1.4 mm thick. The sheets were arranged in stacks containing from 6 to 12 foils of CR39 upstream and downstream of a 12.5 g/cm^2 thick copper target. This arrangement allows to identify the incoming and outgoing projectiles and fragment particles.

After exposure, the CR39 foils were etched in 6.0 N NaOH water solution at (70.0±0.1)°C for 45 hours. The surface areas, eccentricities and the central brightness of the etch-pits were measured with a fully automated Elbek image analyzer system [9]. Background reduction was obtained with quality cuts on the central brightness of the etch-pits and on the eccentricity values.

Figure 1 shows a distribution of the track areas of sulphur ions and their fragments using a single surface measurement . All nuclear fragments with integral charge are clearly resolved with a single measurement of the etch-pits on a single surface. The resulting charge resolution, $\sigma_0 \approx 0.16e$, is clearly inadequate for a search for nuclear fragments with a fractional charge. The resolution σ may be improved by measuring the same track on many surfaces, according to $\sigma = \sigma_0/\sqrt{n}$ where n is the number of independent measurements of the track.

It must be remembered that etch-pit areas increase with increasing ion charges. Thus charge changing nuclear fragmentations may be detected as a change in the area of the etch-pits. The trajectory of each projectile nucleus and of each fragment was reconstructed by tracking the etch cones successively from surface to surface through the CR39 foils before and after the copper target. Small variations of the etch-pit areas from one surface to the other, due to a variety of effects, as for instance batch and etching parameter fluctuations, were corrected by normalizing the peak positions of each successive surface to those on the front surface of the first sheet.

The average surface area of the etch-pits for each fragment plotted versus fragment charge was also used to calibrate the CR39 response [5].

3. CHARGE RESOLUTION AND SEARCH FOR FRACTIONALLY CHARGED NUCLEAR FRAGMENTS

In the search for fragments with fractional charge, the mean etched area was computed as the average over 7 to 12 individual surface measurements for each track. More than 95% of the particles were traced on more than 10 surfaces. Ions which were present in less than 7 surfaces (about 2%) or fragmented in the CR39 were discarded.

Figure 2 shows the charge spectrum of 200 GeV/nucleon sulphur ions and their fragments. The data are relative to 5750 nuclear fragments with $6 \leq Z \leq 15$. The standard deviation of the charge distribution is $\sigma = 0.05e$ for Z=6 and $\sigma \leq 0.07e$ for the other fragments. The slight worsening of the charge resolution with increasing Z is due to the non linear increase of the etch-pit areas with increasing charge.

Similar results are obtained for 14.5 GeV/nucleon silicon ions (see Figure 3) relative to the measurements of 9200 nuclear fragments with charge $7 \leq Z \leq 13$ and for 16 GeV/nucleon oxygen ions, relative to about 4500 nuclear fragments with $6 \leq Z < 8$ (we include the fraction of oxygen ions which lose one neutron).

In Figures 2 and 3 there is no indication of nuclear fragments with fractional charge. From the number of detected fragments we determined upper limits for the production in Cu of fragments with electric charges (integer ±1/3), that is 19/3 up to 46/3 for S, 20/3 up to 40/3 for Si and 17/3 up to 23/3 for O, using the relation

$$F = K(N_C) \,/\, (\varepsilon \; N_F) \;, \qquad (1)$$

where N_C is the number of fragments with charge differing by more than 0.21e from an integer charge in the above intervals, N_F is the number of measured ordinary fragments in the same charge intervals, ε is the product of detection and selection efficiencies of fractionally charged nuclei relative to ordinary nuclei (ε is estimated to be 98% for silicon and sulphur exposures; it is slightly smaller for the oxygen exposure); $K(N_C) = 2.3$ when $N_C = 0$ for the 90% C.L.

There are no candidate events with fractional charge. The upper limit for the production probability in Cu of fragments with fractional charge at 90% C.L. is $F_S \leq 4.1 \times 10^{-4}$ for $17/3 \leq Z \leq 46/3$ in the S case, $F_{Si} \leq 2.6 \times 10^{-4}$ for $20/3 \leq Z \leq 40/3$ in the Si case and $F_O \leq 5.2 \times 10^{-4}$ for $17/3 \leq Z \leq 23/3$ in the O case (see Figure 4). These limits are valid for fractionally charged fragments produced in the Cu target and which lived long enough to penetrate through the copper layer and through at least six CR39 sheets. This requires a minimum path length of 7 mm in CR39 and an average path length of 7 mm in Cu; it corresponds to a time of flight of 4.7×10^{-11} s and a path length of 7.2 g/cm^2.

Since we found no events, we may combine the limits using the formula

$$F = [\,(1/F_S) + (1/F_{Si}) + (1/F_O)]^{-1} \qquad (2)$$

The combined upper limits at 90% C.L. are: $F \leq 2.3 \times 10^{-4}$ for $17/3 \leq Z \leq 20/3$, $F \leq 1.2 \times 10^{-4}$ for $20/3 \leq Z \leq 23/3$ and $F \leq 1.6 \times 10^{-4}$ for $23/3 \leq Z \leq 40/3$. Similar results were obtained by other authors using different beams and different targets [10-12]. In Figure 4 are shown the upper limits from the present work and from ref.12; the limits obtained with very thick Pb targets (10-15 cm) are not included [10,11].

4. FRAGMENTATION CROSS SECTIONS OF $^{28}Si^{14+}$ AND $^{32}S^{16+}$ IN CR39

In order to determine the partial fragmentation cross-sections of ^{28}Si (^{32}S) in CR39 we considered different fragmentation channels for Si (S) nuclei traversing a target of five (eight) sheets of CR39. The ^{28}Si and ^{32}S tracks were selected in the front CR39 sheet, located after the copper target; they were traced through the CR39 foils into the CR39 back sheet. All the undetectable fragments, because of the CR39 threshold at about $Z_t = 5$, were considered as a single fragmentation channel.

Since the sheet thickness is small compared to the mean free path of fragments in CR39, we neglected the double fragmentation process in the foils and we used the simple law

$$\sigma_{CR39}(Z_i,Z_f)= [-1/(K\,t)]\ \ln(1- N_f/N_i), \qquad (3)$$

where $\sigma_{CR39}(Z_i,Z_f)$ is the partial fragmentation cross section in CR39 of a charge Z_i into a fragment of charge Z_f ; K is the number of nuclei / cm^3 of the target, t = 1.4 mm is the mean thickness of each CR39 sheet, N_f is the sum over all CR39 sheets of fragments of charge Z_f formed after each sheet, N_i is the total number of primary ion nuclei reaching each sheet. The tracking efficiency is estimated to be larger than 98%; corrections are smaller than 2%.

The partial cross sections in CR39 for silicon and sulphur ions are given in Table 1 and presented in Figure 5, plotted versus ΔZ, which is the charge difference between the beam ions and the fragments.

The total charge changing fragmentation cross section is given by

$$\sigma_{CR39}= [1/(K\,t)]\ \ln (N_0 / N_1), \qquad (4)$$

where N_0 is the total number of beam ions reaching the first foil of the CR39 stack, N_1 is the number of beam ions which traversed the CR39 stack of thickness t. We obtain:

$$\sigma_{CR39}= (917 \pm 27) \text{ mb for S in CR39}$$

$$\sigma_{CR39} = (839 \pm 26) \text{ mb for Si in CR39.}$$

These results are, within errors, in agreement with previous determinations [13,14]. The measurements show clearly that the partial cross sections $\sigma_{CR39}(Z_i,Z_f)$ for Z_f even are larger than those for Z_f odd.

5. FRAGMENTATION CROSS SECTIONS OF $^{16}O^{8+}$, $^{28}Si^{14+}$ AND $^{32}S^{16+}$ IN Cu

In order to determine the total and partial fragmentation cross sections in the copper target, we reconstructed the trajectories of the beam and of the fragment nuclei through four foil surfaces upstream and four foils downstream of the Cu target. Both the numbers of ions reaching and leaving the Cu target were corrected for the fragmentation in the CR39 foils. The total and partial fragmentation cross sections were calculated using a propagation formula [3,15], which gives the relation between the distributions of the incoming and outgoing particles on the target surfaces

$$N_i(x)=N_i(0)e^{-x\sigma_i}+\sum_{j=1}^{i-1}K_{ij}\,(e^{-x\sigma_i}-e^{-x\sigma_j}) \qquad (5)$$

with

$$K_{ij}=\frac{1}{\sigma_j-\sigma_i}\left[\sigma_{ij}\,N_j(0)-\sum_{n=j+1}^{i-1}\sigma_{in}K_{nj}+\sum_{n=1}^{j-1}\sigma_{ij}K_{jn}\right] \qquad (6)$$

where $x= N_a\rho t / A$, N_a is Avogadro's number, ρ=8.96 g/cm^3 is the copper target density, A=63.5 is the target atomic mass, t =1.4 cm is the target thickness, N_i (0) is the number of nuclear fragments of charge Z_i reaching the target [for the S exposure: i= 1 to 10, corresponding to fragments with Z=16 to 7 ; for the Si exposure: i= 1 to 8 corresponding to Z=14 to 7], N_i (x) is the number of ions of charge Z_i at a depth x in the target, σ_i is the total fragmentation cross-section of ions with charge Z_i, σ_{ij} is the partial fragmentation cross-section of the projectile nucleus of charge Z_j to yield a fragment of charge Z_i. Both cross sections are the sum of the nuclear charge changing cross section σ^n and of the electromagnetic charge changing cross section σ^{em} (this plays an important role in the fragmentation process for very fast ions and high mass targets)[14,16]. For i > 1, (that is for the fragmentation of a fragment), σ_i^n was calculated using the semiempirical formula given by [17]

$$\sigma_i^n = \pi\,[r_0\,(A_p^{1/3}+A_t^{\,1/3}-b)]^2\,, \qquad (7)$$

which fitted the data obtained at 1- 2 GeV/nucleon for projectiles and targets of atomic mass $A_p \geq 12$ and $A_t \geq 12$, respectively; ref.17 gives the numerical values for the parameters r_0 and b: r_0=1.35 fm and b=0.83. The contribution of σ_i^{em} to the total charge changing fragmentation cross section in copper was estimated to be about 10-20%. For j > 1, σ_{ij}^n was computed by scaling the semi-empirical cross section for hydrogen targets to heavier targets[1,2,17]; for ΔZ=1, σ_{ij}^{em} is larger than σ_{ij}^n; with increasing ΔZ, σ_{ij}^{em} decreases more rapidly than σ_{ij}^n. The estimated uncertainty on the calculated total σ_{ij} is about 25%; this means that the uncertainty on the measured partial cross sections is less than 3% .

For the total charge changing fragmentation cross sections in copper we obtained :

for ^{32}S of 200 GeV/nucleon: σ_{Cu} = (3147±40) mb

for ^{28}Si of 14.5 GeV/nucleon: σ_{Cu} = (2446±36) mb

for ^{16}O of 16 GeV/nucleon: σ_{Cu} = (2080± 26) mb

The measured partial cross sections in copper σ_{ij} for silicon and sulphur ions are given in columns 3 and 7 of Table 1 and shown in Figures 6 and 7. The quoted errors are only statistical. A common systematic uncertainty, estimated to be about 4%, has to be added. Within errors, these results agree with previous measurements [13,14,16,19,20], see Figures 6 and 7. We present in Table 1 also the electromagnetic fragmentation cross sections σ_{ij}^{em} (columns 4 and 8) determined by subtracting the pure nuclear cross sections σ_{ij}^{n} from the measured partial cross sections: $\sigma_{ij}^{em} = \sigma_{ij} - \sigma_{ij}^{n}$. The partial nuclear cross sections σ_{ij}^{n} were obtained using the factorization rule[18] $\sigma_{ij}^{n} = \gamma_p^f . \gamma_{pt}$, where γ_p^f is the projectile factor which depends on the type of projectile and target; γ_{pt} is a target factor which depends only on the type of target. Both factors γ_p^f and γ_{pt} were taken from [13,14]. For $\Delta Z < 3$ the electromagnetic dissociation effect is important; for instance, $\sigma_{ij}^{em} \approx \sigma_{ij}^{n}$ for Si nuclei of 14.5 GeV/nucleon and $\Delta Z=1$; $\sigma_{ij}^{em} \approx 2\sigma_{ij}^{n}$ for 200 GeV/nucleon S ions and $\Delta Z = 1$. For $\Delta Z < 7$, the electromagnetic dissociation cross sections decrease exponentially with ΔZ.

As already stated, the data presented here may be used to compute the cross sections in hydrogen nuclei, by using the measured cross sections in CR39 and in carbon. The cross sections in oxygen may be estimated from those in carbon as done in [13-14]. See Table 1 coulumns 5 and 9

6. CONCLUSIONS

We determined the charge resolution of the CR39 made in collaboration with the Intercast Company, to be $\sigma \approx 0.16e$ for a single measurement. From measurements of the same track on 7 to 12 surfaces we obtained a charge resolution $\sigma=0.05e$ at $Z=6$ and $\sigma=0.07e$ at $Z=15$. These are among the best resolutions obtained with this type of detector and also compared to other types of detectors.

We have placed an upper limit for the relative production of nuclear fragments with fractional charge at 2.6×10^{-4} for the Si exposure, 4.1×10^{-4} for the S exposure, 5.2×10^{-4} for the O exposure and 1.2×10^{-4} to 2.3×10^{-4} for the combined exposures [90% C.L.]. These results are compared with previous ones in Figure 4.

We have measured the total and partial charge changing fragmentation cross sections of relativistic oxygen, silicon and sulphur ions in CR39 and Cu targets. The contribution of the electromagnetic dissociation effect was determined for the interactions in Cu; the electromagnetic dissociation plays an important role in the fragmentation involving small charge loss. From the measurements we see that the partial cross sections to obtain even-Z_f fragments are larger than those to obtain odd-Z_f. Within errors, the results are in agreement with previous measurements.

ACKNOWLEDGEMENTS

We would like to thank Drs. P. Baiocchi, G.G. Giani and G. Iori of the Intercast Compagny for their active cooperation. We thank Dr. D. Beavis and the staff of the Brookhaven AGS for the oxygen and silicon exposures, the CERN SPS staff for the sulphur exposure. We acknowledge the contribution of E. Bottazzi, A. Castelvetri, P. Calligola, L. Degli Esposti, M. Folesani, F. Massera, F. Nicoli for the analysis of the CR39 stacks. We acknowledge discussions with C. Brechtmann, B.P. Price and G. Tarlè. We thank the ICTP Programm on Training and Research in Italian Laboratories for providing fellowships.

REFERENCES

[1] R. Silberberg et al., Astrophys. J. Suppl. 25 (1973) 315.

[2] R. Silberberg et al., Astrophys. J. Suppl. 58 (1985) 873.

[3] C. Brechtmann, et al., Nucl. Instr. Meth. B29 (1988) 675.

[4] S.P. Ahlen et al., MACRO collaboration, Nucl. Instr. Meth. A324 (1993) 337.

[5] S. Cecchini, et al., Calibration of the Intercast CR39. Contributed paper to the 16th Int. Conf. on Nuclear Tracks in Solids, Beijing (China), Sept.7-11 (1992). To be published in Nucl. Tracks Radiat. Meas.

[6] A. De Rujula, et al., Phys. Rev. D17 (1978) 285.

[7] G.F. Chapline, Phys. Rev. D25 (1982) 911.

[8] B.A. Arbuzov, et al., Sov. J. Nucl. Phys. 42 (1985) 342.

[9] A. Noll, et al., Nucl. Tracks Radiat. Meas. 15 (1988) 265.

[10] G. Gerbier, et al., Phys. Rev. Lett. 59 (1987) 2535.

[11] A. Hoffmann, et al., Phys. Lett. B 200 (1988) 583.

[12] Y.D. He, et al., Phys. Rev. C 44 (1991) 1672.

[13] C. Brechtmann, et al., Phys. Rev. C 39 (1989) 2222.

[14] C. Brechtmann, et al., Z. Phys. A331 (1988) 463.

[15] O.C. Allkofer et al., Nucl. Phys. B71 (1974) 429.

[16] C. Brechtmann, et al., Z. Phys. A330 (1988) 407.

[17] G.D. Westfall, et al., Phys. Rev. C19 (1979) 1309.

[18] D.L. Olson, et al., Phys. Rev. C28 (1983)1602.

[19] B. Price et al., Phys. Rev. C43 (1991)835.

[20] B. Price et al., Phys. Rev. Lett. 61 (1988) 2193

Z_f	(Si,CR39)	(Si,Cu)	(Si,Cu)	(Si,H) [13]	(S,CR39)	(S,Cu)	(S,Cu)	(S,H) [14]
	$\sigma(Si,Z_f)$ (mb)	σ_{ij} (mb)	σ_{ij}^{em}(mb)	σ_{ij} (mb)	$\sigma(S,Z_f)$ (mb)	σ_{ij} (mb)	σ_{ij}^{em} (mb)	σ_{ij} (mb)
15	-	-	-	-	94±14	494±17	347±22	51.3±6.3
14	-	-	-	-	116±10	361±14	192±19	73.1±7.0
13	78±9	282±14	142±20	62.8±6.3	51±6	158±9	72±12	36.2±4.8
12	84±8	194±10	39±16	58.0±6.5	65±7	168±10	60±14	42.8±5.4
11	48±7	76±8	-3±12	28.5±4.6	34±5	106±8	32±11	23.2±4.0
10	49±7	88±7	2±11	30.5±4.7	52±6	97±7	27±10	23.0±4.0
9	23±5	54±8	5±11	8.5±3.4	24±4	59±6	17±8	15.3±3.2
8	49±6	-	-	30.0±4.9	51±6	115±8	32±11	27.1±4.4
7	41±6	-	-	23.5±4.2	44±6	98±7	31±11	-

Table.1 Partial fragmentation cross sections of 14.5 GeV/nucleon Si and 200 GeV/nucleon S ions in CR39 and in Cu. In columns 2 and 6 are given the measured fragmentation cross sections in CR39; those in copper are given in columns 3 and 7. In columns 4 and 8 are given the electromagnetic fragmentation cross sections in copper computed from the measured cross sections minus the nuclear contributions. In columns 5 and 9 are given the measured fragmentation cross sections in Hydrogen taken from Ref.13 and 14.

FIGURE CAPTIONS

Figure 1 : Etched surface area distribution (in arbitrary units) of 200 GeV/nucleon S^{16+} nuclei and their fragments measured on a single surface of a CR39 foil located immediately downstream of the copper target.

Figure 2 : Charge distribution of 200 GeV/nucleon S^{16+} ions and their fragments based on 7 to 12 surface area measurements for each detected particle. The points in the horizontal axis show the expected positions of the fractional charge nuclei.

Figure 3 : Charge distribution of 14.5 GeV/nucleon Si^{14+} ions and their fragments based on 7 to 12 etched surface area measurements for each detected particle. The points in the horizontal axis show the expected positions of the fractional charge nuclei. The point at Z=6 has not been included.

Figure 4 : Upper limits at 90% C.L. for the production probability of fractionally charged nuclear fragments in heavy ion collisions for the charge interval $5 \leq Z \leq 15$.

Figure 5 : Partial fragmentation cross sections in CR39 for silicon ions of 14.5 GeV/nucleon and sulphur ions of 200 GeV/nucleon into various nuclear fragments for atomic number variation ΔZ ranging from 1 to 9.

Figure 6 : Partial fragmentation cross sections in Cu for silicon ions of 14.5 GeV/nucleon into various nuclear fragments for ΔZ ranging from 1 to 5. Our data are compared to previous results [13,19].

Figure 7 : Partial fragmentation cross sections in Cu for sulphur ions of 200 GeV/nucleon into various nuclear fragments for ΔZ ranging from 1 to 9. Our data are compared to previous results [14,20].

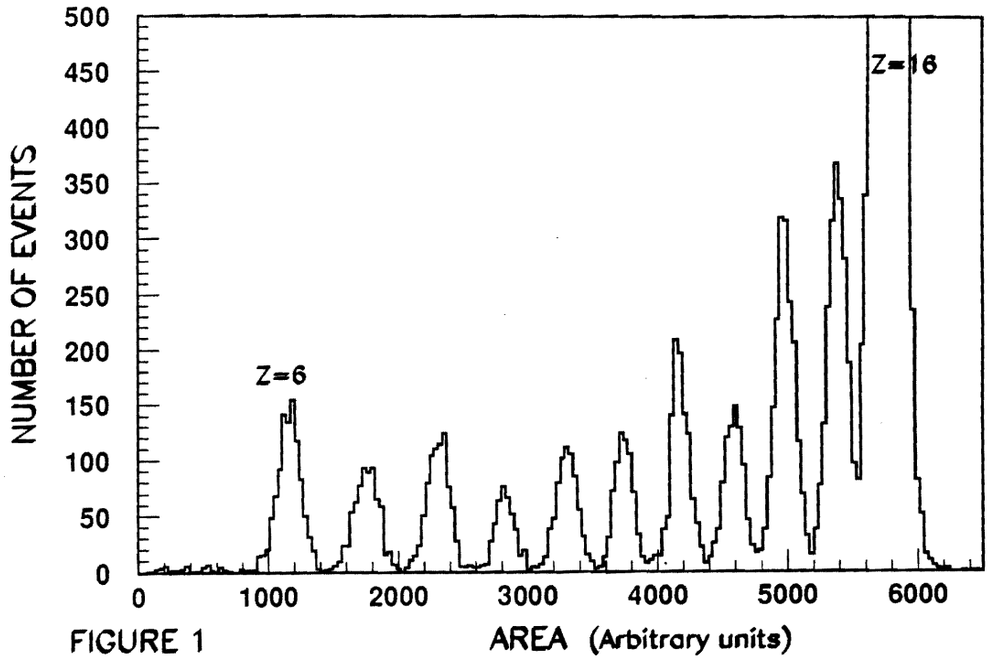
NUMBER OF EVENTS
500
450
400
350
300
250
200
150
100
50
0
Z=6
Z=16
0
1000
2000
3000
4000
5000
6000
AREA (Arbitrary units)

FIGURE 1

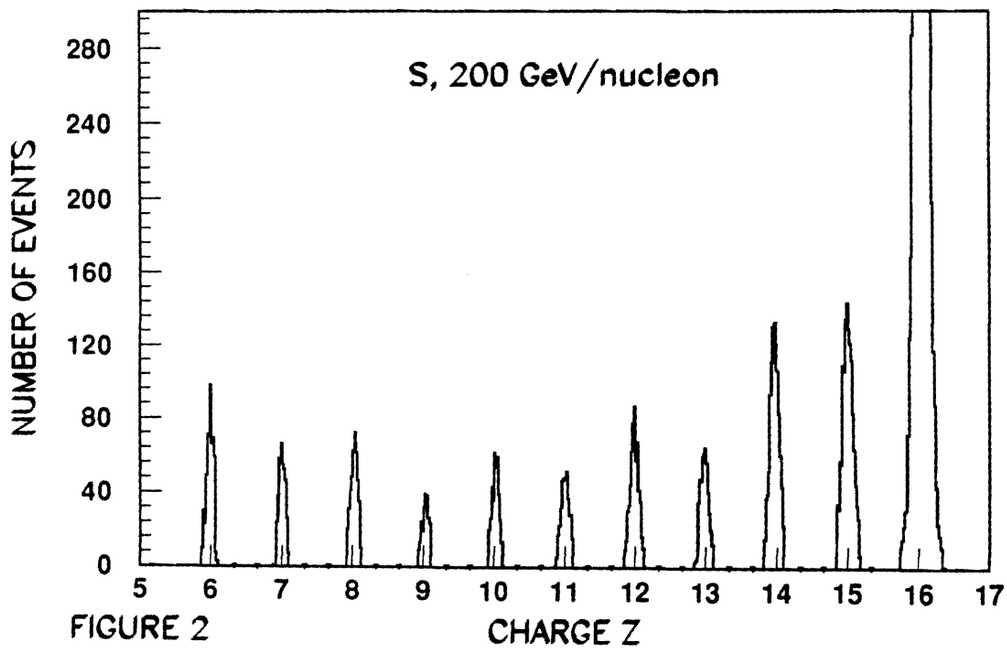

FIGURE 2

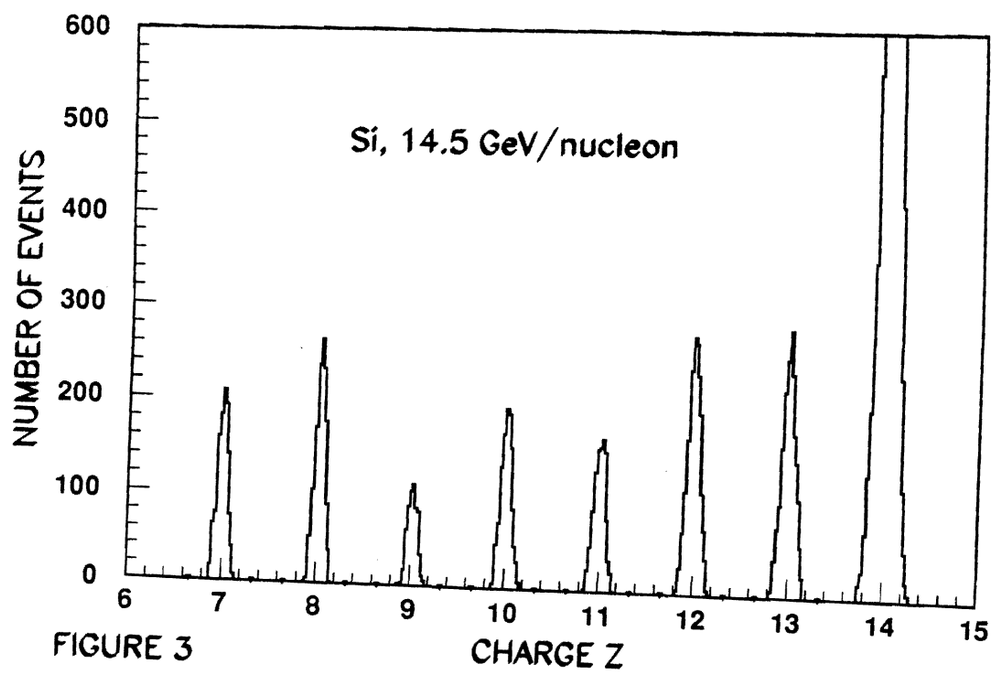

FIGURE 3

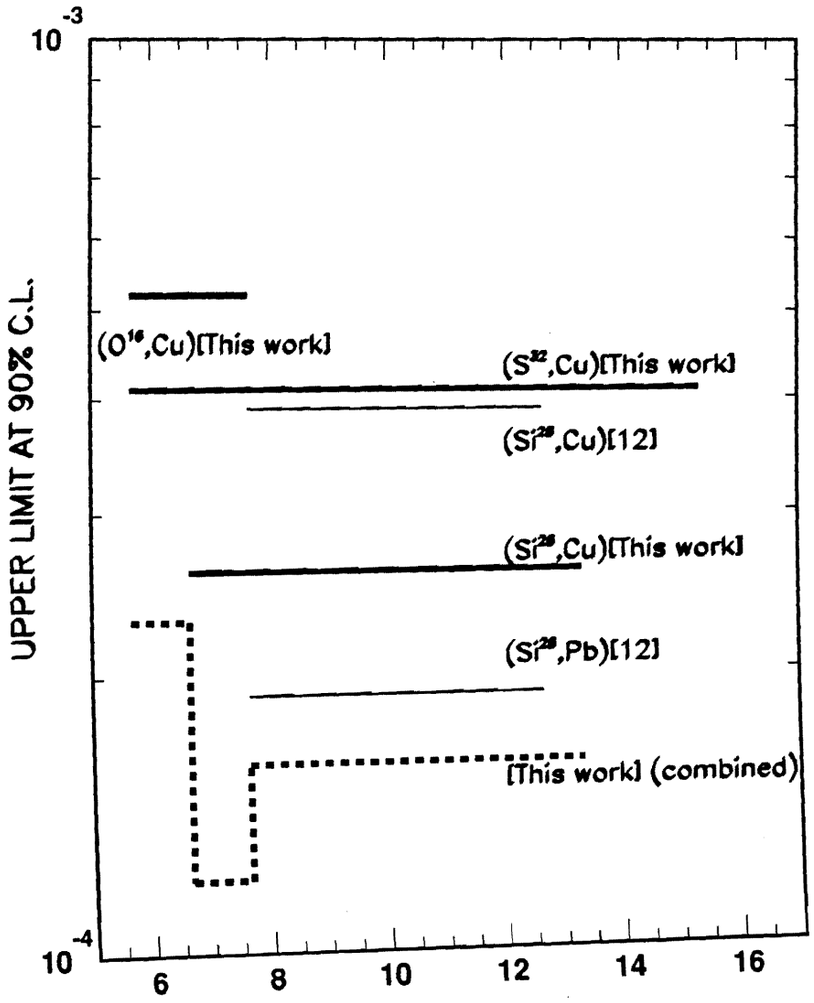
10^{-3}
10^{-4}
UPPER LIMIT AT 90% C.L.
(O^{16},Cu)[This work]
(S^{32},Cu)[This work]
(Si^{28},Cu)[12]
(Si^{28},Cu)[This work]
(Si^{28},Pb)[12]
[This work] (combined)
6
8
10
12
14
16
CHARGE Z

FIGURE 4

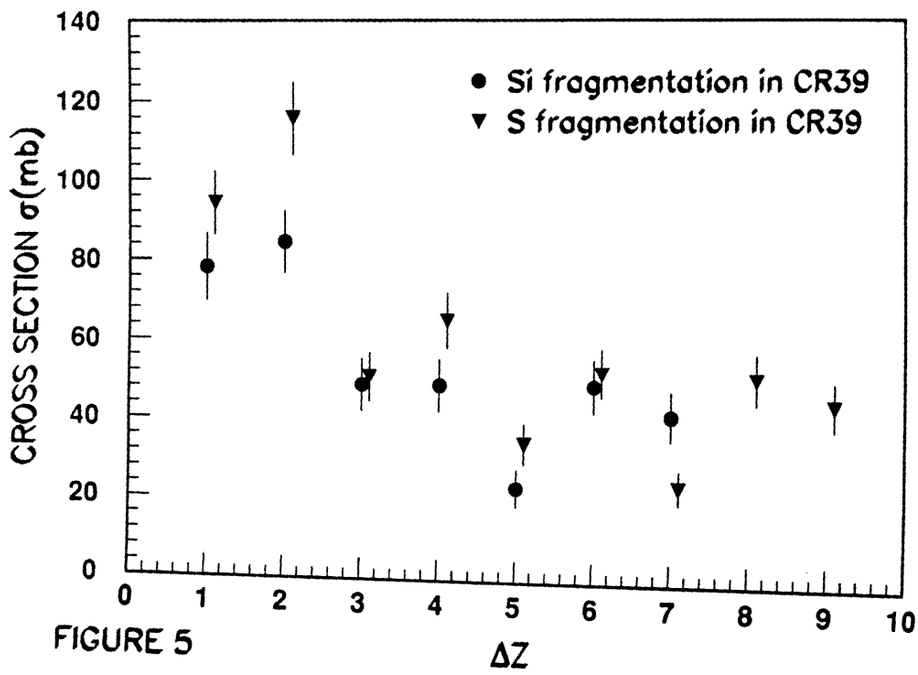
Si fragmentation in CR39
S fragmentation in CR39
CROSS SECTION σ(mb)
ΔZ
0
20
40
60
80
100
120
140
0
1
2
3
4
5
6
7
8
9
10

FIGURE 5

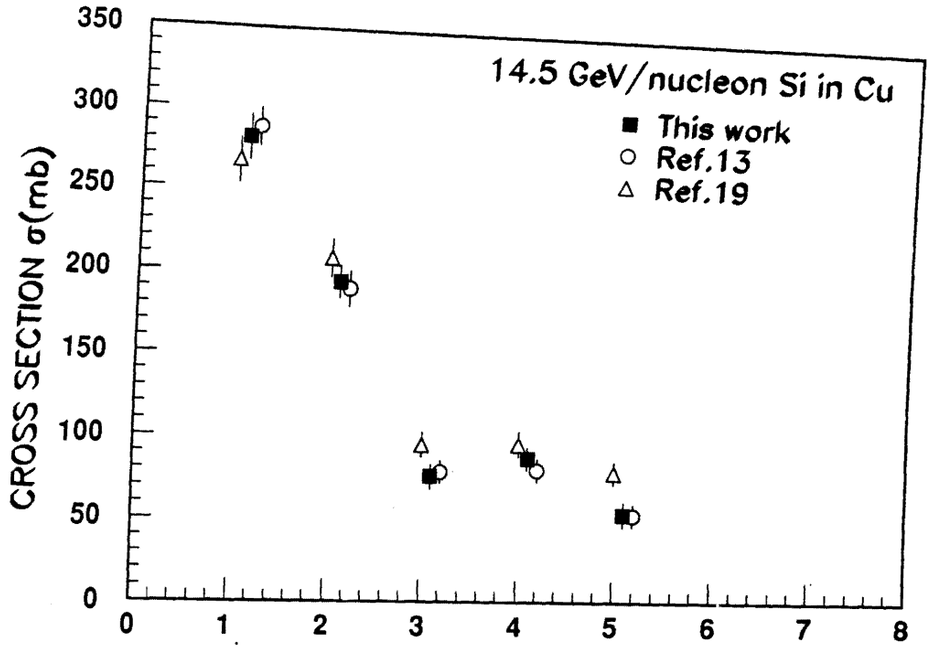

FIGURE 6

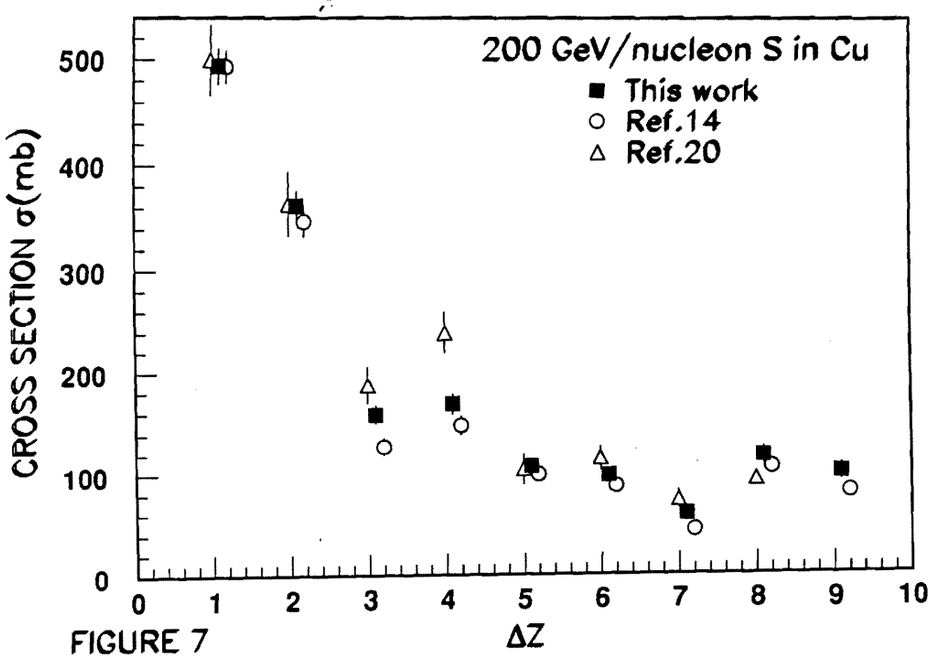

FIGURE 7